# White Matter Hyperintensities in Autopsy-Confirmed Frontotemporal Lobar Degeneration and Alzheimer's Disease

**Philippe Desmarais**
Centre Hospitalier de l'Université de Montréal Centre de Recherche: Centre Hospitalier de l'Universite de Montreal Centre de Recherche
https://orcid.org/0000-0002-7516-9594
**Andrew Gao**
Sunnybrook Health Sciences Centre
**Julia Keith**
Sunnybrook Health Sciences Centre
**Krista Lanctôt**
Sunnybrook Health Sciences Centre
**Ekaterina Rogaeva**
University of Toronto
**Joel Ramirez**
Sunnybrook health sciences centre
**Nathan Herrmann**
Sunnybrook Health Sciences Centre
**Donald T. Stuss**
University of Toronto
**Sandra E. Black**
Sunnybrook Health Sciences Centre
**Mario Masellis** ( mario.masellis@sunnybrook.ca )
Sunnybrook Health Sciences Centre

**Research**

**Keywords:** Alzheimer's disease, Frontotemporal lobar degeneration, White matter hyperintensity, Magnetic resonance imaging, Neuropsychiatric symptoms

**Posted Date:** December 11th, 2020

**DOI:** https://doi.org/10.21203/rs.3.rs-125103/v1



**Version of Record:** A version of this preprint was published at Alzheimer's Research and Therapy on July 13th, 2021. See the published version at https://doi.org/10.1186/s13195-021-00869-6.

## Abstract

Background

We aimed to systematically describe the burden and distribution of white matter hyperintensities (WMH) and investigate correlations with neuropsychiatric symptoms in pathologically proven Alzheimer's disease (AD) and frontotemporal lobar degeneration (FTLD).

Methods

Autopsy-confirmed cases were identified from the Sunnybrook Dementia Study, including 15 cases of AD and 58 cases of FTLD (22 FTLD-TDP cases; 10 FTLD-Tau [Pick's] cases; 11 FTLD-Tau Corticobasal Degeneration cases; and 15 FTLD-Tau Progressive Supranuclear Palsy cases). Data analyses included ANCOVA to compare the burden of WMH on antemortem brain MRI between groups and adjusted linear regression models to identify associations between WMH burden and neuropsychiatric symptoms.

Results

Burden and regional distribution of WMH differed significantly between neuropathological groups ($F_{5,77}$ = 2.67, $P'$ = 0.029), with the FTLD-TDP group having the highest mean volume globally (8,031.50 ± 8,889.15 $mm^3$) and in frontal regions (4,897.45 ± 6,163.22 $mm^3$). The AD group had the highest mean volume in occipital regions (468.25 ± 420.04 $mm^3$). Total score on the Neuropsychiatric Inventory correlated with bilateral frontal WMH volume (β = 0.330, $P$ = 0.006), depression correlated with bilateral occipital WMH volume (β = 0.401, $P$ < 0.001), and apathy correlated with bilateral frontal WMH volume (β = 0.311, $P$ = 0.009), all corrected for the false discovery rate.

Conclusions

These findings suggest that WMH are associated with neuropsychiatric manifestations in AD and FTLD and that WMH burden and regional distribution in neurodegenerative disorders differ according to the underlying neuropathological processes.

## Background

Regional grey matter atrophy has been linked to the clinical expression of Alzheimer's disease (AD) and frontotemporal lobar degeneration (FTLD) [1–3]. Antemortem hippocampal atrophy has been associated with episodic memory deficits [4] while orbitofrontal atrophy has been linked to disinhibition [5]. While regional grey matter atrophy represents an important biomarker for these disorders, these changes occur late in their respective pathological cascades and therefore development of other imaging biomarkers is warranted.

Changes in white matter, such as hyperintensities on T2-weighted MRI sequences, have gained interest as potential biomarkers in neurodegenerative disorders. White matter hyperintensities (WMH) have been associated with cerebrovascular disease and vascular risk factors [6]. More recently, WMH in AD and congophilic amyloid angiopathy (CAA) may represent microvascular dysfunction secondary to amyloid β deposition in the cerebral vasculature [7] as well as venous collagenosis [8]. In prospective longitudinal studies, periventricular WMH correlated negatively with mental processing speed, while left temporal WMH correlated negatively with memory performance [9, 10]. However, neural correlates of WMH have not been extensively and rigorously studied in pathologically-proven cases of AD and FTLD.

Mapping the distribution and burden of WMH in AD and FTLD may further our understanding of the underlying pathological mechanisms of these disorders. In this study, we aimed to describe WMH burden and distribution in these neuropathological entities and investigate neural correlates of neuropsychiatric manifestations.

## Methods

# Participants

This research was carried out as part of the Sunnybrook Dementia Study, a prospective longitudinal cohort study of normal cognitive ageing, mild cognitive impairment, and the most prevalent neurodegenerative dementias conducted at Sunnybrook Health Sciences Centre, University of Toronto (ClinicalTrials.gov: NCT01800214). The design and methods have been previously published [11]. The study was approved by the local research ethics committee and all participants, or their caregivers when appropriate, provided written informed consent, in accordance with the Declaration of Helsinki.

Consecutive deceased participants with autopsy-confirmation of FTLD were retrospectively identified, including cases of FTLD due to Pick's disease (i.e., FTLD-Tau [Pick's]), TDP-43 proteinopathy (i.e., FTLD-TDP), Progressive Supranuclear Palsy (i.e., FTLD-Tau [PSP]), and Corticobasal Degeneration (i.e., FTLD-Tau [CBD]). Cognitively impaired participants with autopsy-confirmation of pure Alzheimer's pathology without other proteinopathies (e.g., synucleinopathy) were consecutively selected. Healthy matched controls were also included for comparison purposes.

# Genetic studies

Genomic DNA was extracted from whole blood using Qiagen kits. DNA from participants with a clinical diagnosis of a frontotemporal dementia spectrum disorder was screened for pathogenic mutations known to cause FTLD: *C9orf72* [12], *GRN* [13], and *MAPT* [14]. A pathogenic expansion of *C9orf72* was considered as having more than 30 repeats. All selected cases of AD were sporadic in nature, free of mutations in the *APP*, *PSEN1*, and *PSEN2* genes [14].

# Neuropathology

Autopsies limited to the brain and spinal cord were performed by an experienced neuropathologist (author JK). Neuropathological diagnoses and staging were made for the primary disease process and any co-existing neurodegenerative phenomena at the time of original autopsy based on a standardized blocking and staining protocol for dementia, applying consensus criteria for AD [15–18] and FTLD [19, 20]. Cases were included in the study and assigned into the following neuropathological diagnostic categories based on the original autopsy reports: (i) AD ($n$ = 15); (ii) FTLD-Tau (Pick's) ($n$ = 10); (iii) FTLD-Tau (PSP) ($n$ = 15); (iv) FTLD-Tau (CBD) ($n$ = 11); and (v) FTLD-TDP ($n$ = 22).

The pathologic classification of FTLD-TDP has evolved in recent years, thus these cases were subjected to a central pathology review. Slides from the original autopsy were retrieved from the Sunnybrook pathology archive and reviewed by authors JK and AG. Additional slides were cut from selected original tissue blocks and stained with antibodies for TDP-43, alpha-synuclein, tau (AT8) and/or p62. Based on this central pathology review, cases within the FTLD-TDP category were re-classified using the Harmonized consensus criteria for FTLD-TDP pathology as types A-D [21, 22].

Cases were excluded from the study if: (i) neuropathological diagnosis could not be accurately assessed; (ii) immunohistochemical staining examination was incomplete and could not be retrospectively completed; and (iii) multiple co-morbid neuropathologies were present, none of which could be assigned unequivocally as the predominant cause of dementia.

## MRI acquisition and analysis

All participants underwent MRI on a 1.5 T GE Signa (Milwaukee, WI, USA) system in compliance with consensus panel imaging recommendations for studies examining vascular cognitive impairment [23]. The following sequences were used for volumetric analysis: T1-weighted-axial three-dimensional (3D) Spoiled Gradient Recalled Echo (SPGR): 5 ms echo time (TE), 35 ms repetition time (TR), 1 number of excitations (NEX), 35$^{o}$ flip angle, 22 × 16.5 cm (FOV), 0.859 × 0.859 mm in-plane resolution, 1.2 to 1.4 mm slice thickness depending on head size-and an interleaved proton density and T2 (interleaved axial dual-echo spin echo: TEs of 30 and 80 ms, 3 s TR, 0.5 NEX, 20 × 20 cm FOV, 0.781 × 0.781 mm in-plane resolution, 3 mm slice thickness).

MR images were analyzed with the semi-automatic brain region extraction (SABRE) and Lesion Explorer (LE) processing pipeline [24], which permits semi-automatized segmentation and parcellation procedures and to obtain regionalized and whole-brain volumetrics for normal appearing tissues and WMH. Volumes for grey matter, normal appearing white matter, and WMH were obtained in 26 regions of interest, 13 per hemisphere. Intracranial volumetric data (grey matter and WMH) were normalized for total intracranial volume (TIV). For analysis, all WMH values were log-transformed after normalizing for TIV due to their known skewed distribution [24].

## Neuropsychological and neuropsychiatric assessments

Participants underwent a standardized clinical evaluation at baseline within 12 weeks of MRI acquisition. This comprised a medical history, physical examination, and a neuropsychological and neuropsychiatric battery [25]. The following vascular risk factors were collected: hypertension, hyperlipidemia, diabetes mellitus, and history of stroke and/or transient ischemic attack. For the purpose of this study, cognitive and neuropsychiatric testing results were retrieved for the following: (i) the Mini-Mental Status Examination (MMSE) [26]; (ii) the Dementia rating scale (DRS) [27]; and (iii) the Neuropsychiatric Inventory (NPI) [28]. For the latter, the total score (maximum of 144 points) and the 12 items, i.e. neuropsychiatric symptom subscores (maximum of 12 points for each item), were obtained.

## Statistical analyses

We compared baseline characteristics between each of the neuropathological groups and the healthy control group using ANOVA with *post hoc* Bonferroni tests for continuous variables, $\chi^2$/Fisher exact tests for categorical/dichotomous variables, respectively, and Kruskal-Wallis with *post hoc* Mann-Whitney U-tests for non-normally distributed data. Differences in total and regional volumes of WMH on T2-weighted imaging among neuropathological groups and the healthy control group were assessed by using ANCOVA, controlling for age at imaging and vascular risk factors. *Post hoc* exploratory evaluation for differences in global WMH volumetrics between FTLD-TDP Harmonized types were also carried out.

We also assessed for the association between regional WMH volumes and corresponding regional grey matter volumes using multiple linear regression analyses, controlling for age, education, sex, and vascular risk factors, with regional WMH volume as the independent variable and the corresponding grey matter volume as the dependent variable.

We conducted linear regressions to assess for associations between global and regional WMH volumes and scores on the NPI (total scores and 12 subscale scores) across all neuropathological groups. For the linear regressions, a model was designed *a priori* and contained age, sex, vascular risk factors, and corresponding regional grey matter volumes as covariates, with WMH volume as the independent variable and NPI score as the dependent variable. The Benjamini-Hochberg procedure was used to control the false discovery rate across all planned correlations and regression analyses, with a false discovery rate (FDR; $Q$) of 0.10. All analyses were thresholded at $P < 0.05$. Statistical analyses were performed with the Statistical Package for the Social Sciences, version 24.0.

### Results

## Participant characteristics

A summary of demographic and clinical characteristics of participants according to neuropathological diagnosis is provided in Table 1 and in the Additional file 1. No significant differences were present except for, as expected, overall performance on the cognitive tests, specifically on the MMSE and on the DRS. These were significantly lower in the neuropathological groups compared to the healthy control group ($F_{5,95}$ = 10.27, $P < 0.0001$, and $F_{5,90}$ = 13.42, $P < 0.0001$,

respectively), but did not differ significantly between neuropathological groups ($F_{4,61}$ = 1.69, $P$ = 0.112 and $F_{4,56}$ = 0.59, $P$ = 0.680 for the mean scores on the MMSE and DRS, respectively). There were six cases of FTLD with pathogenic mutations: 4 *GRN* and 2 *C9orf72* mutation carriers.

Table 1 Demographic and clinical characteristics

| Characteristics | FTLD-TDP (n = 22) | FTLD-tau (Pick's) (n = 10) | FTLD-tau (CBD) (n = 11) | FTLD-tau (PSP) (n = 15) | AD (n = 15) | HC (n = 35) | *P*-values |
|---|---|---|---|---|---|---|---|
| Age at baseline | 66.5 (8.7) | 67.4 (9.6) | 67.4 (6.6) | 71.4 (5.3) | 69.1 (10.0) | 71.2 (7.8) | 0.278 |
| Age at onset of symptoms | 63.2 (8.5) | 63.5 (11.1) | 63.9 (6.0) | 68.3 (5.8) | 65.6 (10.5) | .. | 0.454 |
| Disease duration in years | 3.9 (3.7) | 3.9 (3.7) | 3.6 (1.7) | 3.1 (1.7) | 3.6 (2.2) | .. | 0.903 |
| Female | 10 (45%) | 4 (40%) | 8 (73%) | 6 (40%) | 5 (33%) | 14 (40%) | 0.455 |
| Handedness (R/L/A) | 17/4/1 | 7/2/1 | 10/1/0 | 13/1/1 | 15/0/0 | 16/0/1 | 0.512 |
| Education (yrs) | 15.0 (3.2) | 15.4 (4.1) | 13.5 (3.2) | 15.3 (3.2) | 16.0 (5.5) | 14.4 (3.3) | 0.570 |
| MMSE (/30) | 22.7 (6.3) | 16.9 (10.6) | 21.9 (5.8) | 24.1 (6.2) | 19.9 (6.4) | 28.9 (0.9) | < 0.0001* |
| DRS (/144) | 108.0 (21.1) | 102.6 (36.9) | 103.4 (25.2) | 115.4 (18.9) | 110.9 (21.2) | 140.5 (2.6) | < 0.0001* |
| Vascular risk factors | | | | | | | |
| Hypertension | 6 (27%) | 2 (20%) | 3 (27%) | 5 (33%) | 4 (27%) | 9 (26%) | 0.972 |
| Hyperlipidemia | 5 (23%) | 0 (0%) | 3 (27%) | 2 (13%) | 6 (40%) | 1 (3%) | 0.168 |
| Diabetes mellitus | 0 (0%) | 1 (10%) | 2 (18%) | 0 (0%) | 0 (0%) | 0 (0%) | 0.177 |
| History of stroke/TIA | 2 (10%) | 1 (10%) | 0 (0%) | 0 (0%) | 1 (6.6%) | 0 (0%) | 0.705 |

Data are n (%) and mean (± standard deviation). All percentages were rounded to the nearest whole number.

*Significant difference between groups ($P$ < 0.05) on ANOVA with *post hoc* Bonferroni tests for continuous variables, $\chi^2$/Fisher Exact Tests for categorical/dichotomous variables, respectively, and Kruskal-Wallis with *post hoc* Mann-Whitney U-tests for non-normally distributed data.

*Abbreviations: AD* Alzheimer's disease, *CBD* Corticobasal degeneration, *DRS* Dementia Rating Scale, *FTLD* Frontotemporal lobar degeneration, *HC* Healthy controls, *MMSE* Mini-Mental State Examination, *PSP* Progressive supranuclear palsy, *TIA* Transient ischemic attack.

### Neuropsychiatric symptoms

Baseline neuropsychiatric symptom profile of participants according to neuropathological diagnosis is shown in Fig. 1. Overall score on the NPI differed between groups ($F_{4,45}$ = 4.39, $P$ < 0.001), with FTLD-Tau (Pick's) (42.2 ± 23.7 points) and FTLD-TDP (25.1 ± 10.9 points) having significantly higher mean scores than for the AD group (11.9 ± 8.0 points, $P$ < 0.001 for both comparisons). Apathy was the most prevalent neuropsychiatric manifestation in all neuropathological groups, with 71% of participants having an apathy score ≥ 2 points, while hallucinations and delusions were infrequently reported symptoms. Of all the subgroups, FTLD-Tau due to Pick's disease had the highest caregiver burden mean score (18.2 ± 10.8 points) as well as the highest mean scores for 8 of the 12 NPI subscales.

### WMH volumetrics among neuropathological groups and controls

In the healthy control group, total intracranial WMH and periventricular WMH volumes were significantly associated with age (r = 0.481, $P$ = 0.009 and r = 0.490, $P$ = 0.008, respectively) but not for deep WMH (r = 0.119, $P$ = 0.546). After adjusting for vascular risk factors and age at time of imaging, WMH burden and cerebral distribution significantly differed between neuropathological groups and the healthy control group (Fig. 2). There were significant differences between groups in the total burden of WMH ($F_{5,77}$ = 2.67, $P'$ = 0.029), with FTLD-TDP having the highest mean volume (8,031.50 ± 8,889.15 $mm^3$) and FTLD-Tau (Pick's) having the lowest mean volume (3,088.10 ± 3,238.29 $mm^3$). Groups also differed significantly in volumes of WMH in the periventricular region ($F_{5,77}$ = 2.82, $P'$ = 0.022) and frontal regions ($F_{5,77}$ = 2.59, $P'$ = 0.020), more specifically in lateral frontal regions ($F_{5,77}$ = 2.13, $P'$ = 0.029), with FTLD-TDP having the highest burden in these regions (7,403.87 ± 8,539.13 $mm^3$; 4,897.45 ± 6,163.22 $mm^3$; and 3,761.47 ± 5,068.62 $mm^3$, respectively). The AD group had the highest mean volume of WMH in the occipital region (468.25 ± 420.04 $mm^3$; Fig. 2). *Post hoc* analyses revealed that AD with CAA was associated with significantly higher burden of WMH in the bilateral parietal region than for AD without CAA (3,241.25 ± 2,911.22 $mm^3$ vs. 671.64 ± 663.55 $mm^3$, $P$ = 0.042). For FTLD-TDP, Harmonized type was determined for 19 of 22 cases: type A ($n$ = 11), type B ($n$ = 2), mixed type A + B ($n$ = 2), and type C ($n$ = 4). We did not have adequate power to run statistical analyses due to small FTLD-TDP subgroup sizes, but still compared the WMH volumes visually since this has never been investigated before. Harmonized types A and mixed type A + B had the highest total burden of WMH (10,566.86 ± 10,426.28 $mm^3$) compared to Harmonized types B and C (4,165.08 ± 4,852.29 $mm^3$), as well as in the periventricular region (9,951.27 ± 10,040.96 $mm^3$ vs. 3,507.84 ± 4,282.74 $mm^3$, respectively; Fig. 3 and Fig. 4).

Multiple linear regressions between regional WMH volumes and corresponding grey matter volumes for each neuropathology group and healthy controls were performed. There were no significant associations found in the healthy control and AD groups. In FTLD, increased regional volumes of WMH were associated with decreased volumes of grey matter in the corresponding area in the right frontal region (β = -0.425, $P$ = 0.004), in the right lateral frontal region (β = -0.345, $P$ = 0.034), in the right parietal region (β = -0.299, $P$ = 0.049), and in the right occipital region (β = -0.462, $P$ = 0.002). All of these correlations survived FDR correction.

## Neuropsychiatric symptoms and WMH volumetrics

Across the entire neuropathological cohort, positive associations between neuropsychiatric symptoms and total and regional burden of WMH (Table 2) were observed; specifically, between the total NPI score and WMH volume in frontal regions (bilateral frontal region, β = 0.330, *P* = 0.006), with the strongest correlation found in the right lateral frontal region (β = 0.339, *P* = 0.008). Regarding specific neuropsychiatric manifestations, significant positive correlations were identified for the depression, apathy, and night-time behaviors NPI subscores. For depression, increased bilateral occipital region and right parietal region WMH were associated with higher mean scores (β = 0.401, *P* < 0.001; and β = 0.326, *P* = 0.007, respectively). For apathy, several significant positive correlations were identified with WMH burden in frontal regions, with the strongest correlation being in the bilateral frontal region (β = 0.311, *P* = 0.009). Similarly, several significant positive correlations were identified with night-time behaviors and WMH in frontal regions, with the strongest correlation being in the right lateral frontal region (β = 0.390, *P* = 0.003). These regression analyses were corrected for age, sex, vascular risk factors, and corresponding regional grey matter volumes.

Table 2 Linear regression between white matter hyperintensities and neuropsychiatric symptoms across all subgroups

| **Neuropsychiatric symptom** | **Total NPI** | | **Delusion** | | **Hallucination** | | **Agitation** | | **Depression** | | **Anxiety** | | **Euphoria** | |
|---|---|---|---|---|---|---|---|---|---|---|---|---|---|---|
| **Region** | **β** | p | **β** | P | **β** | p | **β** | p | **β** | p | **β** | p | **β** | p |
| **Total** | 0.212 | 0.080 | 0.138 | 0.271 | -0.116 | 0.358 | 0.077 | 0.540 | 0.267 | 0.028* | 0.056 | 0.653 | 0.109 | 0.37 |
| **Deep matter** | 0.197 | 0.093 | 0.161 | 0.186 | -0.083 | 0.495 | -0.040 | 0.741 | 0.115 | 0.337 | 0.119 | 0.321 | 0.317 | 0.00 |
| **Periventricular** | 0.201 | 0.099 | 0.126 | 0.319 | -0.113 | 0.372 | 0.090 | 0.478 | 0.273 | 0.026* | 0.043 | 0.731 | 0.071 | 0.58 |
| **Frontal** | 0.330 | 0.006* | 0.207 | 0.099 | 0.056 | 0.956 | 0.121 | 0.338 | 0.147 | 0.236 | 0.142 | 0.254 | 0.244 | 0.04 |
| Left | 0.267 | 0.034 | 0.257 | 0.039 | -0.022 | 0.862 | 0.102 | 0.410 | 0.129 | 0.300 | 0.117 | 0.346 | 0.236 | 0.05 |
| Right | 0.282 | 0.017* | 0.148 | 0.253 | 0.042 | 0.741 | 0.106 | 0.409 | 0.138 | 0.279 | 0.129 | 0.303 | 0.191 | 0.12 |
| **Frontal – medial** | 0.089 | 0.493 | -0.085 | 0.531 | 0.135 | 0.314 | 0.019 | 0.892 | -0.054 | 0.688 | -0.008 | 0.951 | 0.232 | 0.08 |
| Left | 0.052 | 0.688 | -0.014 | 0.917 | 0.124 | 0.357 | 0.018 | 0.896 | 0.026 | 0.851 | -0.153 | 0.253 | 0.287 | 0.02 |
| Right | 0.095 | 0.414 | -0.057 | 0.661 | 0.093 | 0.474 | 0.059 | 0.654 | -0.145 | 0.272 | 0.082 | 0.519 | 0.177 | 0.15 |
| **Frontal – lateral** | 0.314 | 0.012* | 0.251 | 0.056 | -0.075 | 0.566 | 0.098 | 0.470 | 0.148 | 0.258 | 0.176 | 0.176 | 0.208 | 0.10 |
| Left | 0.263 | 0.042 | 0.280 | 0.034 | -0.087 | 0.508 | 0.065 | 0.630 | 0.087 | 0.519 | 0.193 | 0.146 | 0.217 | 0.09 |
| Right | 0.339 | 0.008* | 0.225 | 0.097 | -0.027 | 0.839 | 0.097 | 0.484 | 0.250 | 0.067 | 0.172 | 0.200 | 0.192 | 0.15 |
| **Temporal** | 0.078 | 0.509 | 0.090 | 0.462 | -0.097 | 0.426 | 0.034 | 0.782 | 0.166 | 0.166 | 0.095 | 0.426 | -0.155 | 0.19 |
| Left | -0.108 | 0.218 | -0.055 | 0.651 | -0.032 | 0.787 | -0.086 | 0.481 | -0.013 | 0.915 | -0.084 | 0.483 | -0.075 | 0.51 |
| Right | 0.195 | 0.103 | 0.139 | 0.248 | -0.094 | 0.439 | 0.095 | 0.428 | 0.240 | 0.040 | 0.184 | 0.122 | -0.135 | 0.25 |
| **Parietal** | 0.109 | 0.364 | 0.039 | 0.752 | -0.080 | 0.519 | 0.078 | 0.529 | 0.252 | 0.036 | -0.050 | 0.679 | 0.048 | 0.69 |
| Left | 0.097 | 0.423 | 0.053 | 0.663 | -0.070 | 0.567 | 0.125 | 0.303 | 0.120 | 0.319 | -0.038 | 0.728 | 0.044 | 0.71 |
| Right | 0.125 | 0.308 | -0.004 | 0.974 | -0.058 | 0.643 | 0.022 | 0.861 | 0.326 | 0.007* | -0.070 | 0.563 | 0.097 | 0.43 |
| **Occipital** | 0.021 | 0.857 | 0.042 | 0.728 | -0.060 | 0.622 | 0.004 | 0.977 | 0.401 | < 0.001* | -0.050 | 0.675 | -0.094 | 0.42 |
| Left | 0.039 | 0.747 | 0.053 | 0.660 | -0.044 | 0.717 | 0.016 | 0.895 | 0.349 | 0.003* | -0.025 | 0.835 | -0.110 | 0.35 |
| Right | 0.060 | 0.626 | 0.036 | 0.767 | -0.015 | 0.898 | 0.032 | 0.793 | 0.386 | 0.001* | -0.045 | 0.709 | -0.056 | 0.64 |

Associations between regional white matter hyperintensity volumes and neuropsychiatric symptoms were assessed using linear regression analyses. Estimates are presented as standardized β-values to allow for comparison of effect sizes. Model: age, sex, vascular risk factors, and corresponding regional grey matter atrophy as covariates.

*Significant result following Benjamini-Hochberg FDR correction for all correlational tests.

*Abbreviations: FDR* False discovery rate, *NPI* Neuropsychiatric Inventory.

Table 2
Continued

| Neuropsychiatric symptom | Apathy | | Disinhibition | | Aberrant motor | | Irritability | | Night-time behaviors | | Appetite / eating habit changes | |
|---|---|---|---|---|---|---|---|---|---|---|---|---|
| **Region** | **β** | p | **β** | p | **β** | p | **β** | p | **β** | p | **β** | p |
| **Total** | 0.256 | 0.033* | 0.105 | 0.401 | 0.136 | 0.277 | 0.062 | 0.593 | 0.149 | 0.239 | 0.075 | 0.539 |
| **Deep matter** | 0.088 | 0.453 | 0.189 | 0.118 | 0.070 | 0.566 | 0.136 | 0.223 | 0.306 | 0.011* | 0.071 | 0.546 |
| **Periventricular** | 0.265 | 0.028* | 0.086 | 0.494 | 0.138 | 0.275 | 0.047 | 0.687 | 0.116 | 0.363 | 0.070 | 0.564 |
| **Frontal** | 0.311 | 0.009* | 0.181 | 0.150 | 0.241 | 0.052 | -0.013 | 0.913 | 0.322 | 0.010* | 0.237 | 0.049 |
| Left | 0.299 | 0.013* | 0.136 | 0.276 | 0.194 | 0.117 | -0.085 | 0.471 | 0.267 | 0.029 | 0.198 | 0.093 |
| Right | 0.234 | 0.051 | 0.173 | 0.174 | 0.241 | 0.055 | 0.020 | 0.869 | 0.317 | 0.012* | 0.170 | 0.134 |
| **Frontal – medial** | 0.041 | 0.752 | 0.059 | 0.669 | 0.114 | 0.403 | 0.044 | 0.729 | 0.154 | 0.261 | 0.096 | 0.464 |
| Left | 0.077 | 0.561 | 0.029 | 0.829 | -0.051 | 0.708 | -0.003 | 0.979 | 0.215 | 0.113 | -0.002 | 0.990 |
| Right | -0.011 | 0.929 | 0.085 | 0.510 | 0.178 | 0.168 | 0.016 | 0.893 | 0.092 | 0.483 | 0.150 | 0.188 |
| **Frontal – lateral** | 0.308 | 0.013* | 0.161 | 0.230 | 0.225 | 0.087 | -0.060 | 0.628 | 0.313 | 0.017* | 0.196 | 0.122 |
| Left | 0.279 | 0.032* | 0.119 | 0.377 | 0.202 | 0.127 | -0.101 | 0.428 | 0.186 | 0.154 | 0.169 | 0.186 |
| Right | 0.315 | 0.013* | 0.195 | 0.158 | 0.228 | 0.093 | 0.035 | 0.790 | 0.390 | 0.003* | 0.141 | 0.253 |
| **Temporal** | 0.129 | 0.273 | -0.030 | 0.806 | 0.128 | 0.292 | 0.110 | 0.327 | -0.014 | 0.907 | -0.034 | 0.770 |
| Left | -0.047 | 0.695 | -0.079 | 0.511 | -0.011 | 0.925 | -0.028 | 0.802 | -0.066 | 0.585 | -0.100 | 0.404 |
| Right | 0.229 | 0.053 | 0.027 | 0.825 | 0.192 | 0.112 | 0.193 | 0.087 | 0.036 | 0.770 | 0.032 | 0.789 |
| **Parietal** | 0.189 | 0.112 | 0.046 | 0.711 | 0.026 | 0.833 | 0.079 | 0.487 | 0.068 | 0.586 | -0.023 | 0.846 |
| Left | 0.170 | 0.161 | 0.114 | 0.351 | 0.099 | 0.419 | 0.003 | 0.982 | 0.043 | 0.722 | -0.029 | 0.810 |
| Right | 0.191 | 0.111 | 0.009 | 0.942 | -0.020 | 0.873 | 0.138 | 0.226 | 0.120 | 0.341 | 0.012 | 0.921 |
| **Occipital** | 0.065 | 0.581 | -0.024 | 0.843 | -0.022 | 0.857 | 0.146 | 0.189 | -0.094 | 0.442 | -0.139 | 0.232 |
| Left | 0.069 | 0.571 | 0.078 | 0.524 | 0.063 | 0.602 | 0.034 | 0.769 | -0.050 | 0.683 | -0.095 | 0.425 |
| Right | 0.112 | 0.358 | -0.051 | 0.680 | -0.018 | 0.882 | 0.197 | 0.079 | -0.058 | 0.635 | -0.111 | 0.353 |

Associations between regional white matter hyperintensity volumes and neuropsychiatric symptoms were assessed using linear regression analyses. Estimates are presented as standardized β-values to allow for comparison of effect sizes. Model: age, sex, vascular risk factors, and corresponding regional grey matter atrophy as covariates.

*Significant result following Benjamini-Hochberg FDR correction for all correlational tests.

*Abbreviations: FDR* False discovery rate, *NPI* Neuropsychiatric Inventory.

## Discussion

We systematically analysed and compared the volume and distribution of WMH seen on antemortem T2-weighted MRI in a cohort of neuropathologically-proven cases of AD and FTLD, and investigated the brain-behavioral associations between WMH and neuropsychiatric manifestations. We found a differential burden and varying distribution of WMH between these neuropathologies with cases of FTLD-TDP having a notably higher burden of WMH, particularly in frontotemporal regions, and AD cases having a higher burden of WMH in parieto-occipital regions. In AD, concomitant presence of CAA was associated with a higher burden of WMH in the bilateral parietal regions. Moreover, we found that WMH burden correlated negatively with cortical volume in FTLD but not in AD, suggesting potentially different underlying neurobiological mechanisms. Finally, after controlling for several potential confounders, most importantly grey matter atrophy and multiple comparisons, we demonstrated that increased volume of WMH in distinct regions, notably in frontal white matter, was associated with greater neuropsychiatric manifestations as measured by the NPI.

# Mechanisms and distribution of WMH in AD and FTLD

The highest burden of WMH was found in FTLD-TDP cases. Extensive and widespread white matter involvement has been previously described in symptomatic *GRN* mutation carriers without significant vascular risk factors or other white matter diseases [29]. Although anomalies in white matter on diffusion tensor imaging have been described in chromosome 9 open reading frame 72 (*C9orf72)* mutation carriers [30] hyperintensities on T2-weighted or FLAIR imaging in white matter have not been reported for other known FTLD-causing genetic mutations. In the Genetic Frontotemporal Dementia Initiative (GENFI), only symptomatic *GRN* mutation carriers were found to have an increased global load of WMH when compared to normal controls, presymptomatic *GRN* mutation carriers, and both presymptomatic and symptomatic *C9orf72* and *MAPT* mutation carriers [31]. In the symptomatic *GRN* mutation subgroup, increased WMH burden was reported in the frontal and occipital lobes [31]. Although the precise mechanisms leading to white matter lesions in the context of

progranulin deficiency are still not known, it has been hypothesized that progranulin's functions in neuroinflammation and vasoprotection may play pivotal roles [32]. Interestingly in our cohort, FTLD-TDP cases were predominantly sporadic. While the underlying mechanisms leading to preferential involvement of the frontotemporal white matter and related neurocircuits still remain uncertain, the distribution of white matter lesions in our study appears to parallel areas of greater grey matter atrophy, suggesting common pathological factors, such as Wallerian degeneration.

In comparison to FTLD-TDP, FTLD-Tau (Pick`s) had a lower burden of WMH, suggesting that WMH load and distribution could have clinical utility in differentiating between these two proteinopathies that have overlapping clinical presentations. For FTLD-Tau (PSP) and FTLD-Tau (CBD), a few studies have described patterns of white matter atrophy as well as white matter anomalies on DTI [33, 34]. However, these studies have not systematically assessed nor reported the presence of WMH. Increased signal intensity changes on FLAIR images have been described in a small case series of patients with corticobasal syndrome with a higher burden noted more in frontal and parietal subcortical white matter, ipsilateral to the clinically affected hemisphere [35]. However, corticobasal syndrome is a pathologically heterogeneous group with cases due to CBD, PSP, TDP-43, Pick's disease, and AD being described. Interestingly in our cohort, FTLD-Tau (PSP) cases were found to have a significantly higher burden of WMH in parietal regions compared to healthy controls and to have a greater deep white matter burden than CBD cases, findings that have not been previously reported.

In contrast, white matter lesions in AD, such as signal changes and lacunar infarcts [9, 36], have been previously and extensively investigated and appear to be intricately interconnected with AD pathology [37]. WMH in AD have been attributed to periventricular small-vessel disease (SVD) and neurodegenerative changes such as amyloid β deposition in arteries, arterioles, and veins and to contribute independently to brain atrophy and to onset of AD [8, 37]. WMH in AD have also been suggested to result from degenerative axonal loss secondary to cortical hyperphosphorylated tau and amyloid β [38]. Interestingly in our study, higher WMH load in the AD group was not associated with more severe cortical atrophy. Possible explanations for this finding include that WMH in AD may represent cerebral SVD that preferentially affects deep branches, sparing superficial cortical branches early in the course of AD and that we adjusted for age in our model, controlling for the normal cortical atrophy seen with age. Moreover, the preferential distribution of WMH in periventricular regions in AD has been previously hypothesized to be linked to tissue properties such as a relatively lower normal perfusion of this region due to its location in watershed zones [8].

## Neural correlations between WMH and manifestations of AD and FTLD

The significant positive correlations between WMH burden and neuropsychiatric manifestations on the NPI despite adjustment for grey matter volume suggest that WMH are not simply epiphenomena associated with cortical atrophy and that they contribute independently to the clinical manifestations of AD and FTLD. WMH most likely contribute to neuropsychiatric manifestations across these neuropathologies by affecting the organization of networks. Only a few studies have specifically investigated brain-behavior relationships between WMH and neuropsychiatric manifestations in neurocognitive disorders, but no studies were conducted in neuropathologically-proven cases similar to ours. A study in participants with subcortical vascular cognitive impairment and AD reported an association between higher WMH volume in the frontal region with a higher level of apathy [39]. Similarly, a study in participants with probable AD reported increased WMH volumes in frontal regions for patients with apathy and increased WMH volumes in the right parietal region for those with depression [40]. In PSP, behavioral changes measured on the Frontal Behavioral Inventory (FBI) were found to correlate with atrophy in the orbitofrontal cortex and midbrain, but no significant correlations were identified with white matter disease [34]. However, comparable clinico-radiological correlations have been previously described in other neurological disorders, including multiple sclerosis. Findings of these studies highlight the contribution of WMH to neuropsychiatric manifestations across different clinical constructs.

## Strengths and limitations

A main strength of our study is the inclusion of neuropathologically-proven cases of AD and FTLD, including both tau and TDP-43 proteinopathies, which allowed us to study relationships between neuroanatomical locations of WMH and neuropsychiatric manifestations in well-defined neuropathological groups. We were also able to control for several factors associated with WMH in our models. By controlling for regional grey matter atrophy, we assessed the independent contribution of WMH to neuropsychiatric manifestations in these neuropathological entities. Nonetheless, there are limitations to acknowledge. First, genetic mutation carriers constituted only a small proportion of our cohort and therefore our results cannot be generalized to genetic cases of frontotemporal dementia. Hence, we were unable to corroborate the potential differential effects of genetic mutations found in FTLD on neuroimaging findings that have been previously described [31]. As well, cases without co-existing neurodegenerative phenomena were selected for the present study, affecting generalization of findings. While we included a remarkable number of pathology-proven cases, subgroup analyses were limited by the small sample size. Consequently, we could have missed other significant regional differences in WMH volumetrics between subgroups and subgroup-specific neural correlates of neuropsychiatric manifestations. Finally, while we report several statistically significant correlations between WMH volumes, grey matter volumes, and neuropsychiatric manifestations in cross-sectional analyses, the temporal relationships between these variables remains to be further studied using longitudinal data before causation can be firmly ascribed.

## Conclusions

Our findings suggest that WMH seen on T2-weighted brain MRI are associated with neuropsychiatric manifestations in AD and FTLD and that WMH burden and regional distribution in neurodegenerative disorders differ according to the underlying neuropathological processes. WMH could potentially help differentiate between different underlying neuropathologies *in vivo*. Accessible, acceptable, and non-invasive biomarkers are needed in order to improve upon the diagnosis of AD and frontotemporal dementia spectrum disorders, as they remain not uncommonly misdiagnosed in the clinic. Furthermore, WMH could eventually be considered as an interesting surrogate marker for future clinical trials of disease-modifying drugs. Future longitudinal studies need to be conducted to understand the temporal relationship between the occurrence of WMH and presentation with neuropsychiatric symptoms in FTLD and AD.

## Abbreviations

AD: Alzheimer's disease; ANCOVA: Analysis of covariance; ANOVA: Analysis of variance; APP: Amyloid precursor protein; *C9orf72:* Chromosome 9 open reading frame 72; CAA: Congophilic amyloid angiopathy; CBD: Corticobasal degeneration; DRS: Dementia Rating Scale; DTI: Diffusion tensor imaging; FBI: Frontal Behavioral Inventory; FDR: False discovery rate; FTLD: Frontotemporal lobar degeneration; FTLD-Tau: Frontotemporal lobar degeneration due tauopathy; FTLD-TDP: Frontotemporal lobar degeneration due to TDP-43 proteinopathy; GENFI: the Genetic Frontotemporal Initiative; *GRN*: Progranulin gene; HC: Health control; LE: Lesion Explorer; *MAPT*: Microtubule associated protein tau gene; MMSE: Mini-Mental Status Examination; MRI: Magnetic resonance imaging; NPI: Neuropsychiatric Inventory; *PSEN1*: Presenilin-1 gene; *PSEN2*: Presenilin-2 gene; PSP: Progressive supranuclear palsy; SVD: Small-vessel disease; TDP-43: TAR DNA-binding protein 43; TIA: Transient ischemic attack; TIV: Total intracranial volume; WMH: White matter hyperintensity.

## Declarations


### Acknowledgements

PD would like to thank the Fondation du Centre Hospitalier de l'Université de Montréal for supporting his postdoctoral training in Cognitive Neurology. SEB and MM are supported by the Department of Medicine (Sunnybrook Health Sciences Centre and the University of Toronto), the Sunnybrook Foundation, the Hurvitz Brain Sciences Research Program, and the Sunnybrook Research Institute. MM also receives support as co-lead of the Ontario Neurodegenerative Disease Research Initiative funded by the Ontario Brain Institute. We are grateful to Sylvain G. Bélisle for his help with the creation of figures, as well as to Christopher Scott for his support with the processing of brain images. We would also like to acknowledge all of the patients and their families who kindly volunteered to take part in this study and who consented to autopsy.


### Authors' contributions

Concept and design: PD, KL, NH, SEB, and MM; Data acquisition: AG, JK, ER, JR, NH, DTS, SEB, and MM; Statistical analysis: PD and MM; Data interpretation: PD and MM; Drafting of the manuscript: PD, JK, and MM; Obtained funding: SEB and MM; All authors participated in the critical review of the manuscript and approved the submitted version.


### Funding

This work was supported by operating grants from the Canadian Institutes of Health Research to MM and SEB (MOP327387; MOP13129), and from the Weston Brain Institute to MM.


### Competing interests

Dr. Black reports grants and personal fees from Eli Lilly, grants and personal fees from Novartis, grants from GE Healthcare, grants from Biogen, grants from Genentech, grants from Optina, grants and personal fees from Roche, outside the submitted work.

Dr. Masellis reports grants from Canadian Institutes of Health Research, during the conduct of the study; other from Associate Editor, Current Pharmacogenomics and Personalized Medicine, personal fees from Bioscape Medical Imaging CRO, personal fees from GE Healthcare, personal fees from UCB, grants from Canadian Institutes of Health Research, grants from Early Researcher Award, Ministry of Economic Development and Innovation of Ontario, grants from Ontario Brain Institute, grants from Sunnybrook AFP Innovation Fund, grants from Alzheimer's Drug Discovery Foundation (ADDF), grants from Brain Canada, grants from Heart and Stroke Foundation Centre for Stroke Recovery, grants from Weston Brain Institute, personal fees from Novartis, personal fees from Henry Stewart Talks, other from Novartis, grants from Roche, grants from Washington University, grants from Teva, other from Teva, outside the submitted work.

The other authors report no disclosures relevant to the manuscript.

### Ethics approval and consent to participate

The study was approved by the local research ethics committee and all participants, or their caregivers when appropriate, provided written informed consent, in accordance with the Declaration of Helsinki.

### Consent for publication

Not applicable.

### Availability of data and materials

The data that support the findings of this study are available from the corresponding author on reasonable request.

## References


1. Jack CR, Shiung MM, Gunter JL, O'Brien PC, Weigand SD, Knopman DS, et al. Comparison of different MRI brain atrophy, rate measures with clinical disease progression in AD. *Neurology* 2004;62:591-600.
2. Rosen HJ, Gorno-Tempini ML, Goldman WP, Perry RJ, Schuff N, Weiner M, et al. Patterns of brain atrophy in frontotemporal dementia and semantic dementia. *Neurology* 2002;58:198-208.

3. Rohrer JD, Geser F, Zhou J, Gennatas ED, Sidhu M, Trojanowski JQ, et al. TDP-43 subtypes are associated with distinct atrophy patterns in frontotemporal dementia. *Neurology* 2010;75:2204-11.
4. Chetelat G, Desgranges B, de la Sayette V, Viader F, Berkouk K, Landeau B, et al. Dissociating atrophy and hypometabolism impact on episodic memory in mild cognitive impairment. *Brain* 2003;126:1955-67.
5. Finger E, Zhang J, Dickerson B, Bureau Y, Masellis. Disinhibition in Alzheimer's disease is associated with reduced right frontal pole cortical thickness. *J Alzheimers Dis* 2017;60:1161-70.
6. Ylikoski A, Erkinjuntti T, Raininko R, Sarna S, Sulkava R, Tilvis R. White-matter hyperintensities on MRI in the neurologically nondiseased elderly - analysis of cohorts of consecutive subjects aged 55 to 85 years living at home. *Stroke* 1995;26:1171-77.
7. Gurol ME, Irizarry MC, Smith EE, Raju S, Diaz-Arrastia R, Bottiglieri T, et al. Plasma beta-amyloid and white matter lesions in AD, MCI and cerebral amyloid angiopathy. *Neurology* 2006;66:23-9.
8. Keith J, Gao F, Noor R, Kiss A, Balasubramaniam G, Au K, et al. Collagenosis of the deep medullary veins: An underrecognized pathologic correlate of white matter hyperintensities and periventricular infarction? *J Neuropathol Exp Neurol* 2017;76:299-312.
9. Ramirez J, McNeely AA, Scott CJM, Stuss DT, Black SE. Subcortical hyperintensity volumetrics in Alzheimer's disease and normal elderly in the Sunnybrook Dementia Study: correlations with atrophy, executive function, mental processing speed, and verbal memory. *Alzheimers Res Ther* 2014;6:49.
10. Smith EE, Salar DH, Jeng J, McCreary CR, Fischl B, Schmahmann JD, et al. Correlations between MRI white matter lesion location and executive function and episodic memory. *Neurology* 2011;76:1492-9.
11. Nestor SM, Mišić B, Ramirez J, Zhao J, Graham SJ, Verhoeff NPLG, et al. Small vessel disease is linked to disrupted structural network covariance in Alzheimer's disease. *Alzheimers Dement* 2017;13:749-60.
12. Xi Z, Zinman L, Grinberg Y, Moreno D, Sato C, Bilbao JM, et al. Investigation of c9orf72 in 4 degenerative disorders. *Arch Neurol* 2012:69;1583-90.
13. Masellis M, Momeni P, Meschino W, Heffner Jr R, Elder J, Sato C, et al. Novel splicing mutation in the progranulin gene causing familial corticobasal syndrome. *Brain* 2006;129:3115-23.
14. Farhan SMK, Dilliot AA, Ghani M, Sato C, Liang E, Zhang M, et al. The ONDRISeq panel: custom-designed next-generation sequencing of genes related to neurodegeneration. *NPJ Genom Med* 2016;1:16032.
15. Braak H, Alafuzoff I, Arzberger T, Kretzschmar H, Del Tredici K. Staging of Alzheimer disease-associated neurofibrillary pathology using paraffin sections and immunocytochemistry. *Acta Neuropathol* 2006;112:389-404.
16. Alafuzoff I, Arzberger T, Al-Sarraj S, Bodi I, Bogdanovic N, Braak H, et al. Staging of neurofibrillary pathology in Alzheimer's disease: a study of the BrainNet Europe Consortium. *Brain Pathol* 2008;18:484-96.
17. Hyman BT, Phelps CH, Beach TG, Bigio EH, Cairns NJ, Carrillo MC, et al. National Institute on Aging-Alzheimer's Association guidelines for the neuropathologic assessment of Alzheimer's disease. *Alzheimers Dement* 2012;8:1-13.
18. Montine TJ, Phelps CH, Beach TG, Bigio EH, Cairns NJ, Dickson DW, et al. National Institute on Aging-Alzheimer's Association guidelines for the neuropathologic assessment of Alzheimer's disease: a practical approach. *Acta Neuropathol* 2012;123:1-11.
19. Cairns NJ, Bigio EH, Mackenzie IRA, Neumann M, Lee VMY, Hatanpaa KJ, et al. Neuropathologic diagnostic and nosologic criteria for frontotemporal lobar degeneration: consensus of the Consortium for Frontotemporal Lobar Degeneration. *Acta Neuropathol* 2007;114:5-22.
20. Mackenzie IRA, Neumann M, Bigio EH, Cairns NJ, Alafuzoff I, Kril J, et al. Nomenclature for neuropathologic subtypes of frontotemporal lobar degeneration: consensus recommendations. *Acta Neuropathol* 2009;117:15-8.
21. Mackenzie IRA, Neumann M, Baborie A, Sampathu DM, Du Plessis D, Jaros E, et al. A harmonized classification system for FTLD-TDP pathology. *Acta Neuropathol* 2011;122:111-3.
22. Neumann M, Mackenzie IRA. Review: Neuropathology of non-tau frontotemporal lobar degeneration. *Neuropathol Appl Neurobiol* 2019;45:19-40.
23. Hachinski V, Iadecola C, Petersen RC, Breteler MM, Nyenhuis DL, Black SE, et al. National Institute of Neurological Disorders and Stroke-Canadian Stroke Network vascular cognitive impairment harmonization standards. *Stroke* 2006;37:2220-41.
24. Ramirez J, Gibson E, Quddus A, Lobaugh NJ, Feinstein A, Levine B, et al. Lesion Explorer: a comprehensive segmentation and parcellation package to obtain regional volumetrics for subcortical hyperintensities and intracranial tissue. *Neuroimage* 2011;54:963-73.
25. Misch MR, Mitchell S, Francis PL, Sherborn K, Meradje K, McNeely AA, et al. Differentiating between visual hallucination-free dementia with Lewy bodies and corticobasal syndrome on the basis of neuropsychology and perfusion single-photon emission computed tomography. *Alzheimers Res Ther* 2014;6:71.
26. Folstein MF, Folstein SE, McHugh PR. "Mini-mental state". A practical method for grading the state of patients for the clinician. *J Psychiatr Res* 1975;12:189-98.
27. Mattis S. Dementia Rating Scale. Professional manual. Florida: Psychological Assessment Resources 1988.
28. Cummings JL. The Neuropsychiatric Inventory: Assessing psychopathology in dementia patients. *Neurology* 1997;48:S10-S16.
29. Caroppo P, Le Ber I, Camuzat A, Clot F, Naccache L, Lamari F, et al. Extensive white matter involvement in patients with frontotemporal lobar degeneration; Think progranulin. *JAMA Neurol* 2014;71:1562-6.
30. Papma JM, Jiskoot LC, Panman JL, Dopper EG, den Heijer T, Donker Kaat L, et al. Cognition and gray and white matter characteristics of presymptomatic C9orf72 repeat expansion. *Neurology* 2017;89:1-9.
31. Sudre CH, Bocchetta M, Cash D, Thomas DL, Woolacott I, Dick KM, et al. White matter hyperintensities are seen only in GRN mutation carriers in the GENFI cohort. *NeuroImage: Clinical* 2017;15:171-80.

32. Ahmed Z, Mackenzie IRA, Hutton ML, Dickson DW. Progranulin in frontotemporal lobar degeneration and neuroinflammation. *J Neuroinflammation* 2007;4:7.
33. Boxer AL, Geschwind MD, Belfor N, Gorno-Tempini ML, Schaeur GF, Miller BL, et al. Patterns of brain atrophy that differentiate corticobasal degeneration syndrome from progressive supranuclear palsy. *Arch Neurol* 2006;63:81-6.
34. Cordato NJ, Duggins AJ, Halliday GM, Morris JGL, Pantelis C. Clinical deficits correlate with regional cerebral atrophy in progressive supranuclear palsy. *Brain* 2005;128:1259-66.
35. Koyama M, Yagishita A, Nakata Y, Hayashi M, Bandoh M, Mizutani T. Imaging of corticobasal degeneration syndrome. *Neuroradiology* 2007;49:905-12.
36. Englund E. Neuropathology of white matter changes in Alzheimer's disease and vascular dementia. *Dement Geriatr Cogn Disorder* 1998:9(suppl 1):6-12.
37. Alosco ML, Sugarman MA, Besser LM, Tripodis Y, Martin B, Palmisano J, et al. A clinicopathological investigation of white matter hyperintensities and Alzheimer's disease neuropathology. *J Alzheimers Dis* 2018;63:1347-60.
38. McAleese KE, Firbank M, Dey M, Colloby SJ, Walker L, Johnson M, et al. Cortical tau load is associated with white matter hyperintensities. *Acta Neuropathol Commun* 2015;3:60.
39. Kim HJ, Kang SJ, Kim C, Kim GH, Jeon S, Lee JM, et al. The effects of small vessel disease and amyloid burden on neuropsychiatric symptoms: a study among patients with subcortical vascular cognitive impairments. *Neurobiol aging* 2013;34:1913-20.
40. Starkstein SE, Mizrahi R, Capizzano AA, Acion L, Brockman S, Power BD, et al. Neuroimaging correlates of apathy and depression in Alzheimer's disease. *J Neuropsychiatry Clin Neurosci* 2009;21:259-65.


## Figures

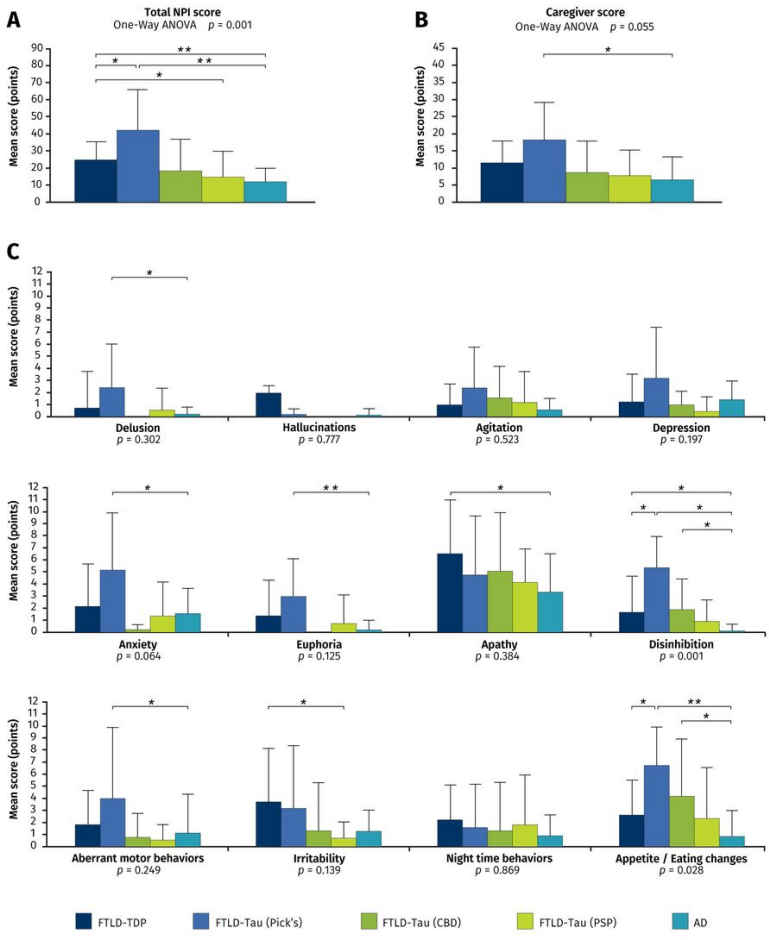


**Figure 1**

Neuropsychiatric symptoms at baseline. Mean score and standard deviation on the Neuropsychiatric Inventory (NPI) for all of the pathological subgroups. (A) Total NPI score. (B) Caregiver score. (C) Subscale items. P-values for differences between subgroups (ANOVA) are found underneath graphs. All bars in the figure are significant differences between each pair with * = P < 0.05 and ** = P < 0.005. Abbreviations: AD Alzheimer's disease, CBD Corticobasal degeneration, FTLD Frontotemporal lobar degeneration, PSP Progressive Supranuclear Palsy.

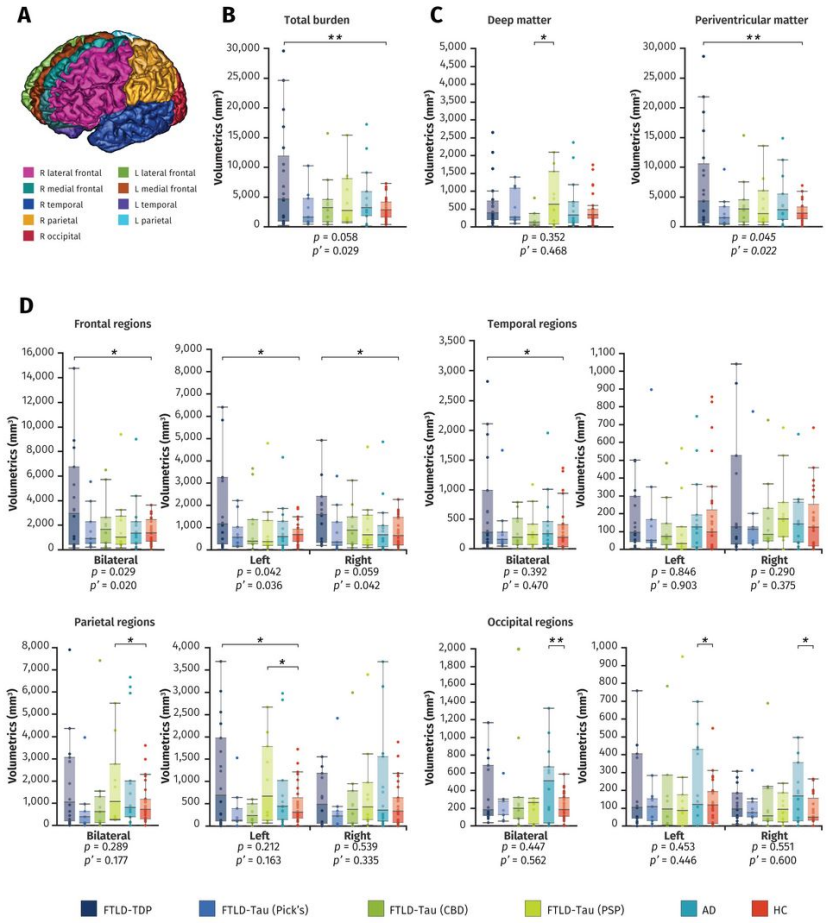


## Figure 2

Comparison of white matter hyperintensity volumes between groups. Box plots show white matter hyperintensity volumes on T2-weighted images according to neuropathological diagnosis, with lower and upper hinges of each boxplot corresponding to 25th and 75th percentiles of data. (A) SABRE parcellation of brain regions. (B) Total intracranial white matter burden. (C) Deep white matter and periventricular white matter burden. (D) Regional volumetrics. Underneath the graphs are P-values for differences between subgroups (ANOVA) and P'-values for differences between subgroups adjusting for age and vascular risk factors (ANCOVA). All bars in the figure are significant differences between each pair with * = P < 0.05 and ** = P < 0.005. Abbreviations: AD Alzheimer's disease, CBD Corticobasal degeneration, FTLD Frontotemporal lobar degeneration, HC Healthy controls, PSP Progressive Supranuclear Palsy.

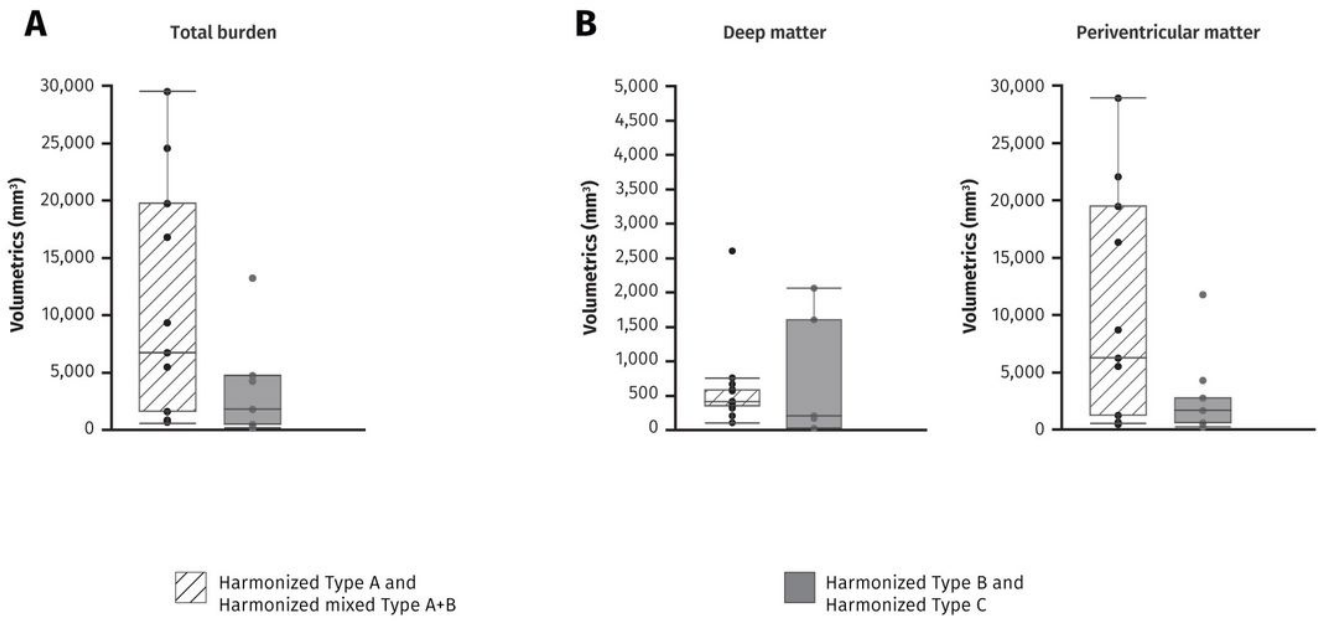


Figure 3

Comparison of white matter hyperintensity volumes according to Harmonized types. Box plots show white matter hyperintensity volumes on T2-weighted images according to neuropathology diagnosis, with lower and upper hinges of each boxplot corresponding to 25th and 75th percentiles of data. (A) Total intracranial white matter burden. (B) Deep white matter and periventricular white matter burden.

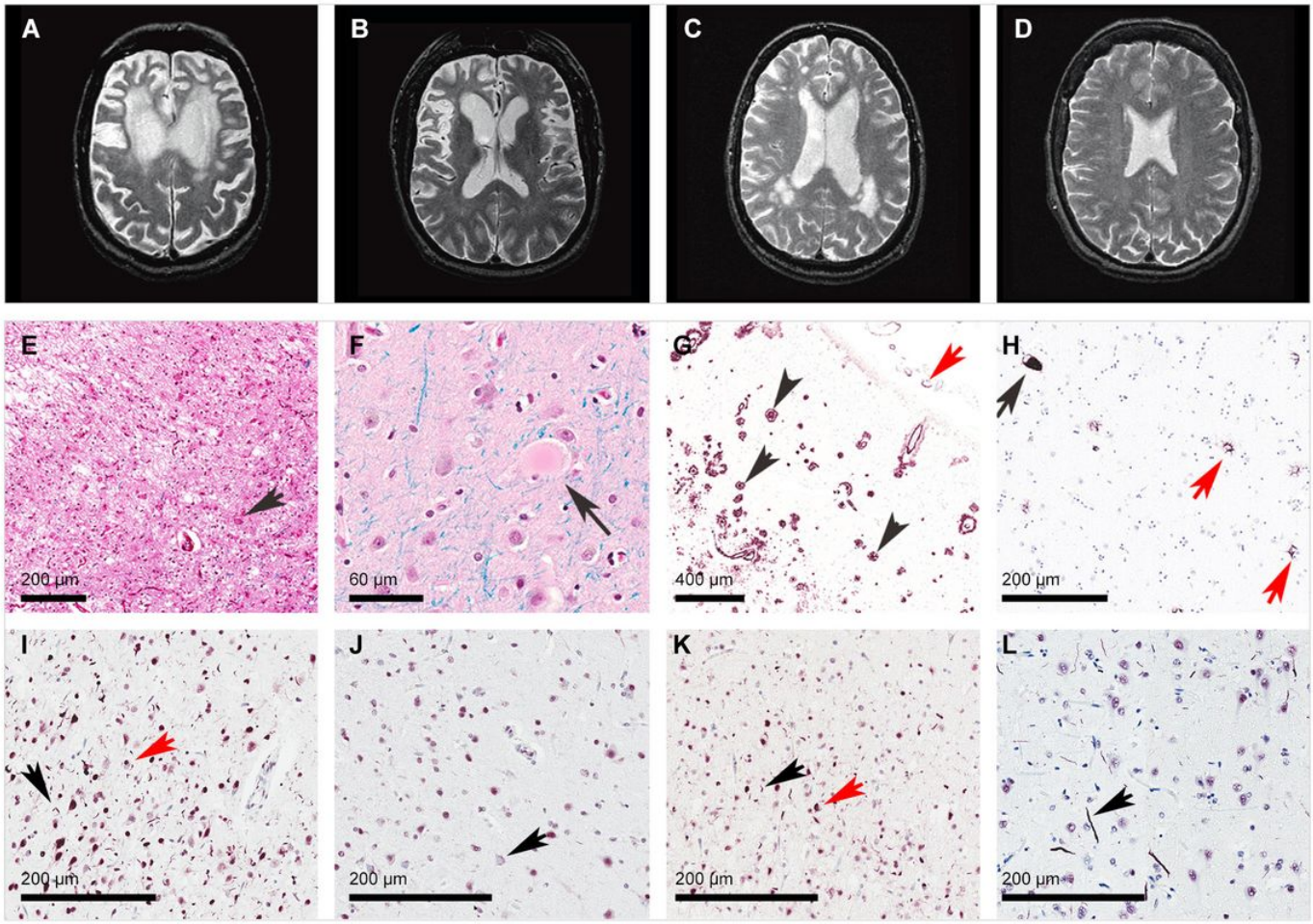


**Figure 4**

Selected examples of T2-weighted axial images and neuropathological findings of included participants. (A) T2-MRI of FTLD-TDP case with severe burden of WMH and prominent atrophy in medial and dorsolateral prefrontal cortex bilaterally; (B) T2-MRI of FTLD-tau case with prominent atrophy in medial and dorsolateral prefrontal cortex bilaterally with little WMH; (C) T2-MRI of AD case with WMH in posterior regions; and (D) T2-MRI of a healthy control. (E) H&E staining of FTLD-tau (Pick's) case showing severe neuronal loss and gliosis in frontal cortex with a ballooned neuron (black arrow); (F) H&E staining of FTLD-tau (CBD) case showing a ballooned neuron (black arrow) in frontal cortex; (G) beta-amyloid immunostaining of AD case showing frequent neuritic amyloid plaques (black arrows) and amyloid angiopathy (red arrow) in frontal cortex; and (H) tau (AT8) immunostaining of FTLD-tau (PSP) case showing a neurofibrillary tangle (black arrow) and astrocytic inclusions (red arrows). (I) FTLD-TDP Harmonized type A with short dystrophic neurites (black arrow) and compact neuronal cytoplasmic inclusions (red arrow) preferentially located in superficial cortical layers. (J) FTLD-TDP Harmonized type B with diffuse granular neuronal cytoplasmic inclusions (black arrow). (K) Mixed FTLD-TDP Harmonized A+B type with superficial dystrophic neurites (black arrow) and compact neuronal cytoplasmic inclusions (red arrow). (L) FTLD-TDP Harmonized type C with long thick dystrophic neurites (black arrow). Abbreviations: AD Alzheimer's disease, CBD Corticobasal degeneration, FTLD Frontotemporal lobar degeneration, PSP Progressive Supranuclear Palsy.

## Supplementary Files

This is a list of supplementary files associated with this preprint. Click to download.

- Additionalfile1.docx